Comptes Rendus
Géoscience — Sciences de la Planète
Supplementary material to the article available at:
https://doi.org/10.5802/crgeos.230

Supplementary material: First evidence of sinter and travertine in Cameroon: fault reactivation and geothermal implications

Milan Stafford Tchouatcha [*, a], **Arnaud Patrice Kouske** [b], **Primus Azinwi Tamfuh** [c, d], **Alain Préat** [e], **René Toyama** [f], **Roger Feumba** [g], **Vannelle Tiokeng Ngounfack** [a], **Vivant Madjingain** [h], **Yaya Berinyuy Konglim** [a] **and Rigobert Tchameni** [h]

[a] Department of Earth Sciences, Faculty of Science, University of Dschang, P.O. Box 67, Dschang, Cameroon

[b] University Institute of Technology, University of Douala, P.O. Box 8698, Douala, Cameroon

[c] Department of Soil Science, Faculty of Agronomy and Agricultural Sciences, University of Dschang, P.O. Box 222, Dschang, Cameroon

[d] Department of Mining and Mineral Engineering, National Higher Polytechnic Institute, University of Bamenda, P.O. Box 39, Bambili, Cameroon

[e] Res. Grp. - Biogeochemistry and Modeling of the Earth System - Sedimentology and Basin Analysis, University of Brussels, Av. F-D Roosevelt 50, B-1050, Brussels, Belgium

[f] Department of Earth Sciences, Faculty of Science, University of Bangui, P.O. Box 908, Bangui, Central African Republic

[g] Department of Earth Sciences, Faculty of Science, University of Yaoundé I, P.O. Box 812, Yaoundé, Cameroon

[h] Department of Earth Sciences, Faculty of Science, University of Ngaoundéré, P.O. Box 454, Ngaoundéré, Cameroun

E-mails: inter_milanac@yahoo.fr (M. S. Tchouatcha), arnaudpatricek@gmail.com (A. P. Kouske), aprimus20@yahoo.co.uk (P. A. Tamfuh), alainpreat@icloud.com (A. Préat), toyamarene@gmail.com (R. Toyama), rfeumba2002@gmail.com (R. Feumba), ngounfackvanelle@gmail.com (V. T. Ngounfack), madjingainvivant@gmail.com (V. Madjingain), berinyuyyaya@gmail.com (Y. B. Konglim), rigotchameni@yahoo.fr (R. Tchameni)

* Corresponding author.

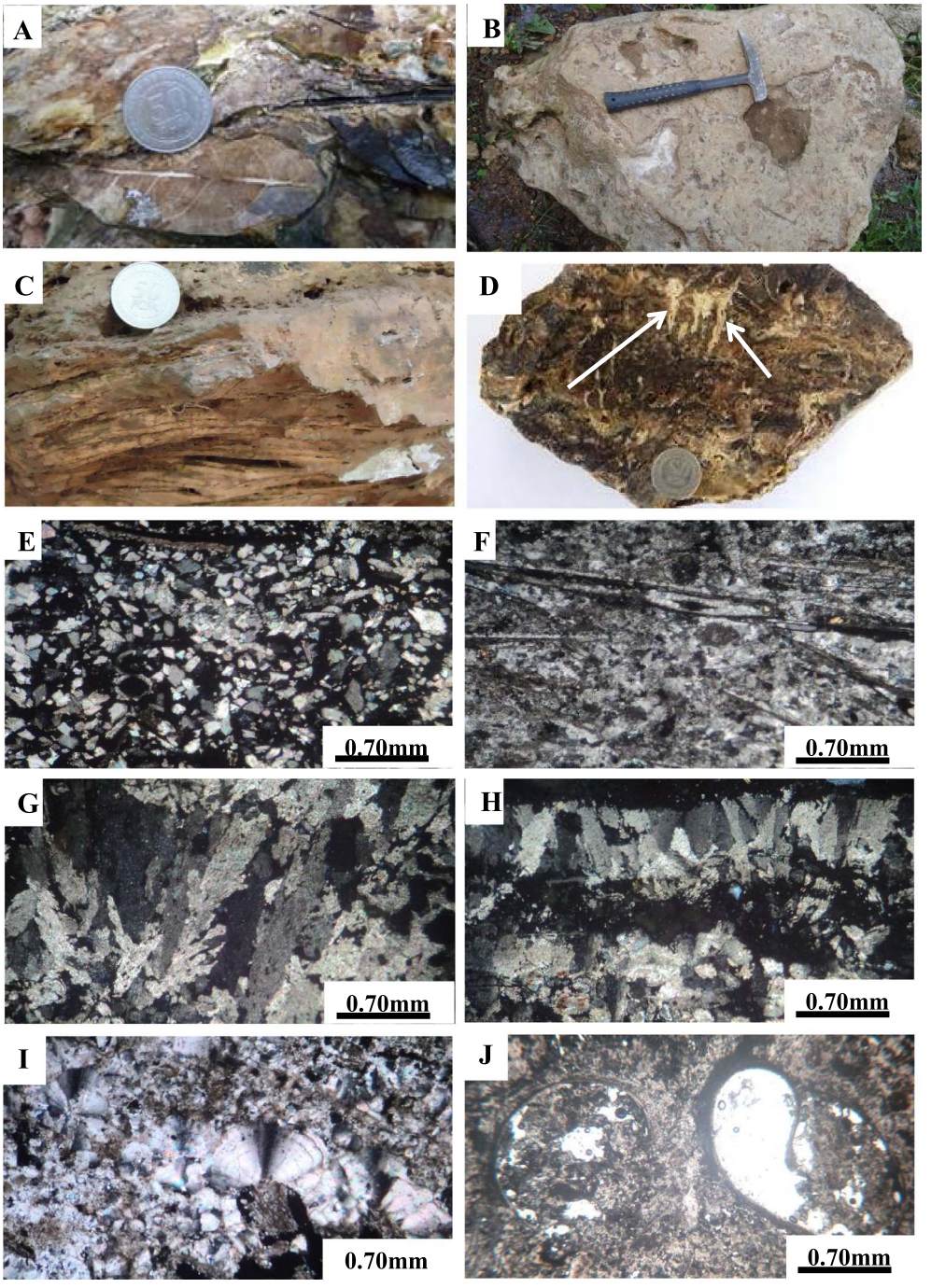

Supplementary Figure S1. Lithofacies and microphotographs of main microstructures of precipited deposits; (A) Detail showing the calcareous siliceous sinter outcrop with stacked leafs; (B) Residual block of whitish compact travertine with dissolution prints; (C) Cross-laminations with elongated voids; (D) Rough bedded brownish-darkish siliceous sinter with affected by vertical mud cracks with calcite filling veins (E) Clastic sparite crystals without any particular arrangement, random distribution; (F) Bioclastic microstructure (plant-rich); (G) Lamellar sparite crystals (PL); (H) Infra-millimetre- to millimetre-thick laminae alternation of clotted sparite and micrite (PL); (I) Radial siliceous fan with syntaxial acicular needles; (J) Bioclastic microstructure with association of ostracod and gastropod in a siliceous matrix.

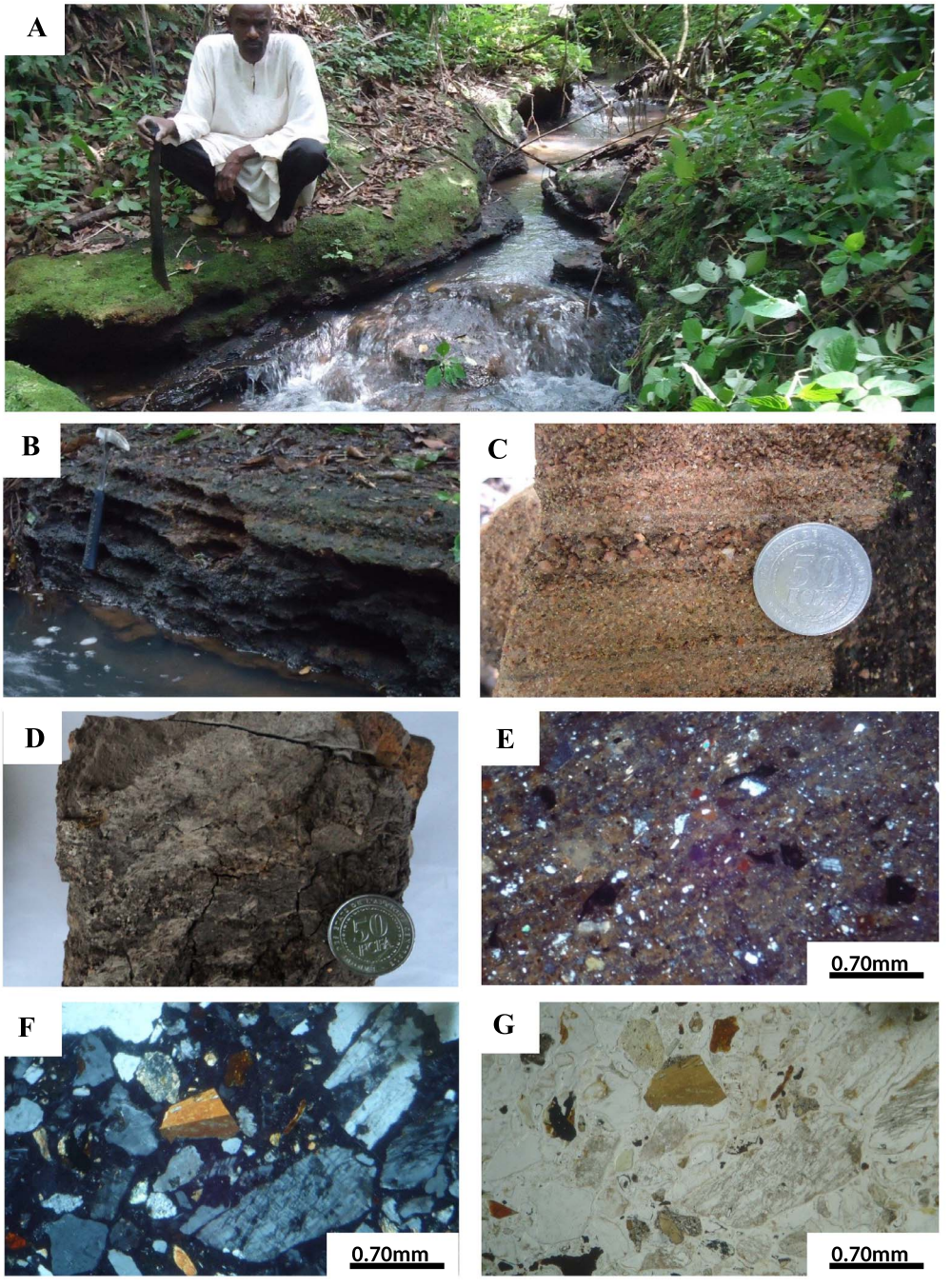

Supplementary Figure S2. Lithofacies and microphotographs of main microstructures of detrital deposits; (A) Basal deposit incised by Mambere stream and widely buried by vegetation and soil; (B) Bedded basal conglomerate; (C) Bedded and laminated sandstone; (D) Dark grey claystone hand specimen; (E) Very fine to fine clastics (quartz and clay) in a heterogranular matrix (Sandy claystone, PL); (F) Median to very coarse poorly sorted clastic grained (quartz, plagioclases, microcline and hormblende) in a (conglomeratic sandstone, PL); (G) Colorless siliceous sinter cement in the conglomeratic sandstone (PPL).

Supplementary Table S1. Major elements composition (wt. %) and elemental ratios of the studied samples and average compositions of PAAS

	Samples																		
	Travertines				Siliceous to calcareous siliceous sinter								Detrital deposits					Standard	
	TLT01	TLT1	TLT2	TLT3	TLT02	TLT0	TLT04	TLAS	TLAS1	TLALI	TLTSB	TLTSV	TLAN	TLMGF	TLMAG	TLANb	TLMAGb	TLMGFb	DL	PAAS
SiO_2	39.06	9.08	12.32	22.17	93.71	94.37	95.77	94.74	94.79	90.22	66.33	63.22	53.81	76.93	73.39	54.31	80.4	75.39	0.01	62.8
Al_2O_3	0.02	0.09	0.1	0.1	0.05	0.21	0.08	0.23	0.1	1.78	0.05	0.07	19.45	8.42	10.92	20.14	7.76	9.29	0.01	18.9
Fe_2O_3	0.4	0.44	0.59	0.68	0.41	0.05	0.19	0.96	1.18	1.87	0.26	2.06	4.7	3.19	1.99	5.05	1.6	3.13	0.04	6.5
MgO	1.56	2.26	2.17	2.04	0.13	0.13	0.05	0.04	0.11	0.08	0.62	0.76	0.9	0.67	0.39	0.92	0.27	0.71	0.01	2.2
CaO	30.8	46.98	44.8	39.31	1.48	0.77	0.26	0.09	0.08	0.12	16.11	16.29	0.71	0.97	0.48	0.73	0.38	1.05	0.01	1.3
Na_2O	0.01	0.04	0.04	0.04	<0.01	0.02	0.01	<0.01	<0.01	0.04	0.03	0.05	0.21	0.78	0.16	0.23	0.16	0.79	0.01	1.2
K_2O	<0.01	0.01	0.01	0.03	<0.01	0.01	0.01	0.05	0.01	0.21	0.01	0.04	1.24	4.29	0.95	1.3	0.85	4.3	0.01	3.7
TiO_2	<0.01	0.01	0.01	0.01	<0.01	0.01	<0.01	0.02	<0.01	0.13	<0.01	<0.01	2.34	0.85	1.27	2.45	0.79	0.96	0.01	1
P_2O_5	0.04	0.03	0.02	0.04	0.01	0.01	0.02	0.02	0.03	0.03	0.02	0.03	0.1	0.14	0.05	0.1	0.04	0.16	0.01	0.16
MnO	0.18	0.06	0.11	0.06	0.01	<0.01	<0.01	<0.01	<0.01	<0.01	0.05	0.04	0.02	0.06	0.02	0.02	0.01	0.06	0.01	0.11
Cr_2O_3	<0.002	<0.002	<0.002	<0.002	<0.002	<0.002	<0.002	0.002	<0.002	0.004	<0.002	<0.002	0.062	0.016	0.051	0.061	0.038	0.018	0.002	—
LOI	27.8	40.7	39.5	35.3	4.2	4.4	3.6	3.8	3.7	5.5	16.4	17.3	16.1	3.3	10.1	14.3	7.5	3.8	−5.1	—
SUM	99.87	99.7	99.72	99.78	100	99.99	99.99	99.952	100	99.984	99.88	99.86	99.642	99.616	99.771	99.73	99.89	99.82	−4.968	—

The PAAS values are cited from Taylor and McLennan [1985] and McLennan [2001].

Supplementary Table S2. Trace elements composition (ppm) and elemental ratios of the studied samples and average composition of PAAS

	Samples																			
	Travertines				Siliceous to calcareous siliceous sinters								Detrital deposits						Standard	
	TLT01	TLT1	TLT2	TLT3	TLT02	TLT0	TLT04	TLAS	TLAS1	TLALI	TLTSB	TLTSV	TLAN	TLMGF	TLMAG	TLANb	TLMAGb	TLMGFb	DL	PAAS
Ba	24	228	197	177	8	13	32	30	40	104	91	100	534	1622	403	590	374	1692	1	650
Ni	31	<20	<20	<20	<20	<20	<20	<20	<20	<20	<20	<20	112	37	134	114	72	35	20	55
Sc	<1	<1	<1	<1	<1	<1	<1	<1	<1	2	<1	<1	20	5	11	21	7	6	1	16
Be	11	8	7	10	2	4	2	15	6	5	12	13	17	8	27	13	7	8	1	—
Co	11.3	0.4	0.2	0.6	4.8	3.8	3.6	0.9	1.2	2.3	0.6	0.4	12.6	11.4	46.8	12.2	13.7	11.4	0.2	23
Cs	0.2	0.4	0.6	0.6	0.2	0.3	0.3	1.3	0.4	6.9	0.3	0.7	9.8	2.8	14.9	9.5	12.6	5.7	0.1	5.16
Ga	<0.5	<0.5	<0.5	<0.5	<0.5	<0.5	<0.5	<0.5	<0.5	2.8	<0.5	0.7	28.7	9.7	14.3	26.6	8.7	10.1	0.5	20
Hf	<0.1	0.1	<0.1	0.1	<0.1	0.5	<0.1	0.4	0.1	0.5	0.1	0.1	16.3	6.6	13.3	16.5	10.7	10.2	0.1	5
Nb	0.3	0.4	0.4	0.2	0.4	0.7	0.6	1.6	1	4.3	0.8	1	63	19.7	35.5	66.9	21.6	22.1	0.1	19
Rb	0.4	0.9	1.1	2.3	0.4	0.8	0.5	3	1.2	14.4	0.8	3.4	65.6	141.2	47.6	67.7	40.5	146.7	0.1	160
Sn	<1	<1	<1	<1	2	<1	<1	<1	2	<1	<1	<1	3	1	2	4	1	2	1	—
Sr	818	2304.1	2042.2	1832.5	172.9	109.7	30.6	17.5	29.3	54.9	940.3	923.7	230.4	442.3	215.3	233.2	184.1	455.9	0.5	200
Ta	<0.1	<0.1	<0.1	<0.1	<0.1	<0.1	<0.1	<0.1	<0.1	0.4	<0.1	<0.1	3.9	1.1	2	4	1.4	1.4	0.1	1.28
Th	<0.2	<0.2	<0.2	<0.2	<0.2	<0.2	<0.2	0.3	<0.2	3.2	<0.2	<0.2	30.1	12	13.2	30.6	9.4	15.4	0.2	14.6
U	8.1	1.3	1.1	1.9	13.3	12.4	7.1	4	6.7	6.6	2.3	1.1	8.3	3	9.3	7.7	12.1	3.5	0.1	3.1
V	33	<8	<8	<8	15	11	14	<8	<8	14	<8	<8	185	106	119	178	86	104	8	150
W	<0.5	<0.5	<0.5	<0.5	1	<0.5	<0.5	<0.5	1.4	<0.5	<0.5	0.6	1.7	0.7	1.4	1.8	1.1	3.5	0.5	—
Zr	2.1	4	5.7	4.3	2.1	19.4	3.3	20.6	5.8	26.2	8.2	3.4	659.9	255.9	544.5	682	404.5	421.2	0.1	210
Y	2	0.6	0.8	0.7	0.9	0.3	0.4	0.6	0.4	1.7	3	2.6	43.2	11	16.4	43.4	10.4	13.7	0.1	27

The PAAS values are cited from Taylor and McLennan [1985] and McLennan [2001].

Supplementary Table S3. Rare-earth elements composition (ppm) and elemental ratios of the studied samples and average composition of PAAS and Chondrites

	Samples																		Standard		
	Travertines				Siliceous to calcareous siliceous sinters								Detrital deposits								
	TLT01	TLT1	TLT2	TLT3	TLT02	TLT0	TLT04	TLAS	TLAS1	TLALI	TLTSB	TLTSV	TLAN	TLMGF	TLMAG	TLANb	TLMAGb	TLMGFb	DL	PAAS	Chondrites
La	2.4	0.9	0.9	0.7	1.3	0.3	0.9	1.6	1.4	7.3	1	0.9	110.7	36.9	43.5	115	25.3	42.8	0.1	38.2	0.237
Ce	2.5	1.3	1.5	1.3	1.1	0.5	1	1.9	1.5	9.5	2.1	1.4	199.8	63.9	85.1	214.7	48.5	74.8	0.1	79.6	0.613
Pr	0.17	0.19	0.21	0.17	0.09	0.02	0.12	0.21	0.15	1.34	0.21	0.19	22.85	7.63	8.91	24.26	5.14	9.1	0.02	8.83	0.093
Nd	0.8	0.5	0.6	0.3	0.4	<0.3	0.5	0.7	0.5	4.9	0.9	0.6	83.7	28.4	32.4	88.8	19.1	31.6	0.3	33.9	0.457
Sm	0.23	0.1	0.08	0.05	0.08	<0.05	0.09	0.13	0.08	0.72	0.17	0.1	14.68	4.56	5.71	14.95	3.27	5.44	0.05	5.55	0.148
Eu	0.04	0.03	0.04	<0.02	0.02	<0.02	0.02	0.02	0.03	0.15	0.05	0.05	3.53	1.1	1.3	3.57	0.76	1.32	0.02	1.08	0.056
Gd	0.36	0.07	0.14	0.07	0.15	0.07	0.1	0.15	0.15	0.65	0.29	0.2	11.74	3.5	4.45	12.2	2.59	4.05	0.05	4.66	0.199
Tb	0.04	0.02	0.02	0.01	0.02	<0.01	0.01	0.02	0.01	0.07	0.04	0.04	1.54	0.46	0.62	1.63	0.36	0.54	0.01	0.77	0.036
Dy	0.25	0.11	0.11	0.09	0.09	<0.05	0.06	0.13	0.12	0.32	0.39	0.28	8.14	2.24	3.36	8.81	1.98	2.78	0.05	4.68	0.246
Ho	0.07	<0.02	0.03	0.02	<0.02	<0.02	<0.02	<0.02	<0.02	0.04	0.06	0.07	1.54	0.4	0.59	1.63	0.4	0.53	0.02	0.99	0.055
Er	0.2	0.05	0.07	0.05	0.04	0.03	<0.03	0.07	0.05	0.15	0.26	0.24	4.33	1.16	1.68	4.27	1.08	1.44	0.03	2.85	0.16
Tm	0.03	<0.01	0.02	<0.01	<0.01	<0.01	<0.01	0.01	<0.01	0.02	0.04	0.03	0.57	0.17	0.24	0.62	0.15	0.21	0.01	0.41	0.025
Yb	0.23	<0.05	0.07	0.05	0.07	<0.05	<0.05	0.08	<0.05	0.18	0.25	0.27	3.84	1.17	1.67	3.95	1.13	1.34	0.05	2.82	0.161
Lu	0.03	0.01	0.02	0.02	<0.01	<0.01	<0.01	0.01	<0.01	0.02	0.04	0.03	0.54	0.17	0.28	0.57	0.19	0.21	0.01	0.43	0.025
Eu/Eu*	0.54	1.69	1.78	1.59	0.86	1.59	0.99	0.67	1.29	1.03	1.06	1.66	1.27	1.30	1.21	1.24	1.23	1.32	—	0.65	—
Ce/Ce*	0.90	0.73	0.80	0.87	0.74	1.49	0.70	0.76	0.76	0.70	1.06	0.78	0.92	0.88	1.00	0.94	0.98	0.87	—	1.05	—

The PAAS values are cited from Taylor and McLennan [1985] and McLennan [2001];

$Eu/Eu^* = (Eu_{sample}/Eu_{PAAS})/(Sm_{sample}/Sm_{PAAS})^{1/2}(Gd_{sample}/Gd_{PAAS})^{1/2}$;

$Ce/Ce^* = (Ce_{sample}/Ce_{PAAS})/(La_{sample}/La_{PAAS})^{1/2}(Pr_{sample}/Pr_{PAAS})^{1/2}$.

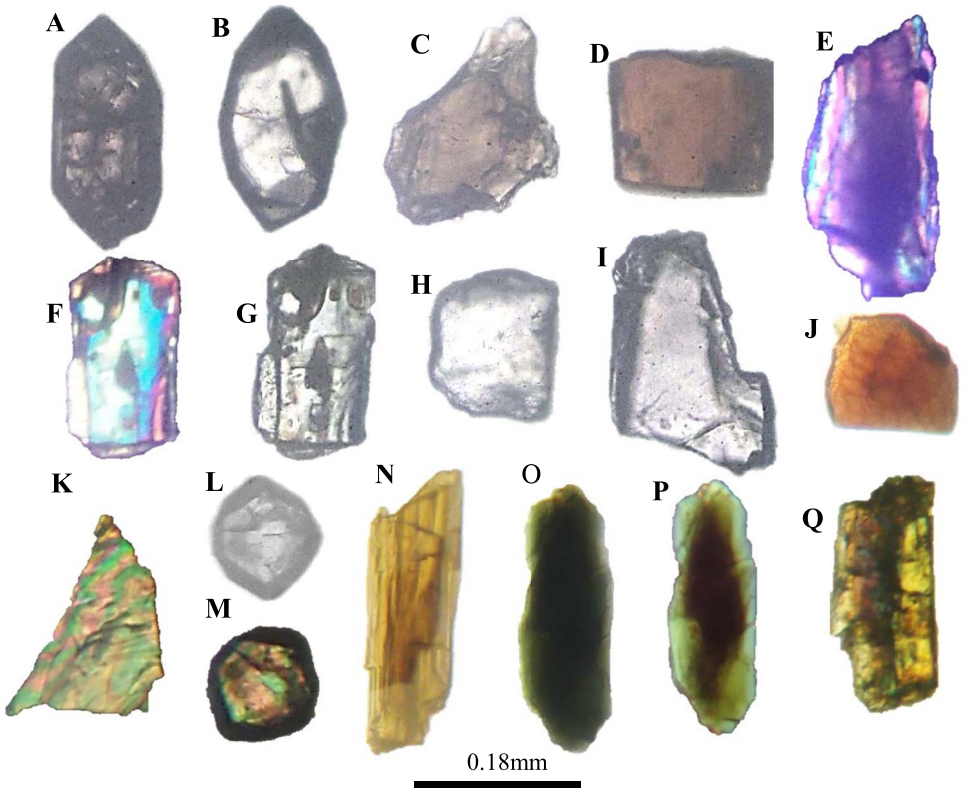

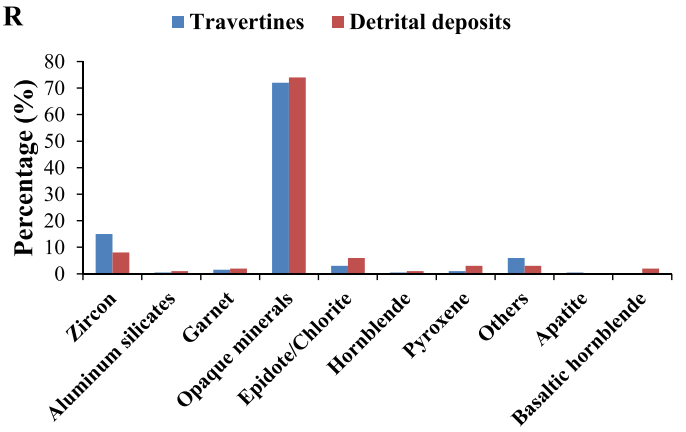

Supplementary Figure S3. Microphotographs of selected detrital heavy minerals; A–I from travertine deposits and J–Q from detrital deposits, and their concentration and comparison in the different studied group facies (L): A = Zoned zircon (PPL); B = Unzoned zircon (PPL); C = Clinopyroxene (PPL); D = Tourmaline (PPL); E– Hornblende; F– Kyanite (PL); G = Kyanite (PPL); H = Apatite (PPL), I = Colorless garnet (PPL); J = Brown garnet (PPL); K = clinozoisite (PL); L = Sub-rounded zircon (PPL); M = Sub-rounded zircon (PL); N = Brown epidote (Allanite, PPL); O = Green epidote (Pistacite, PPL); P = Green epidote (PL); Q = Basaltic horblende (PL); R: Proportions and correlation between heavy minerals from travertine and detrital deposits.

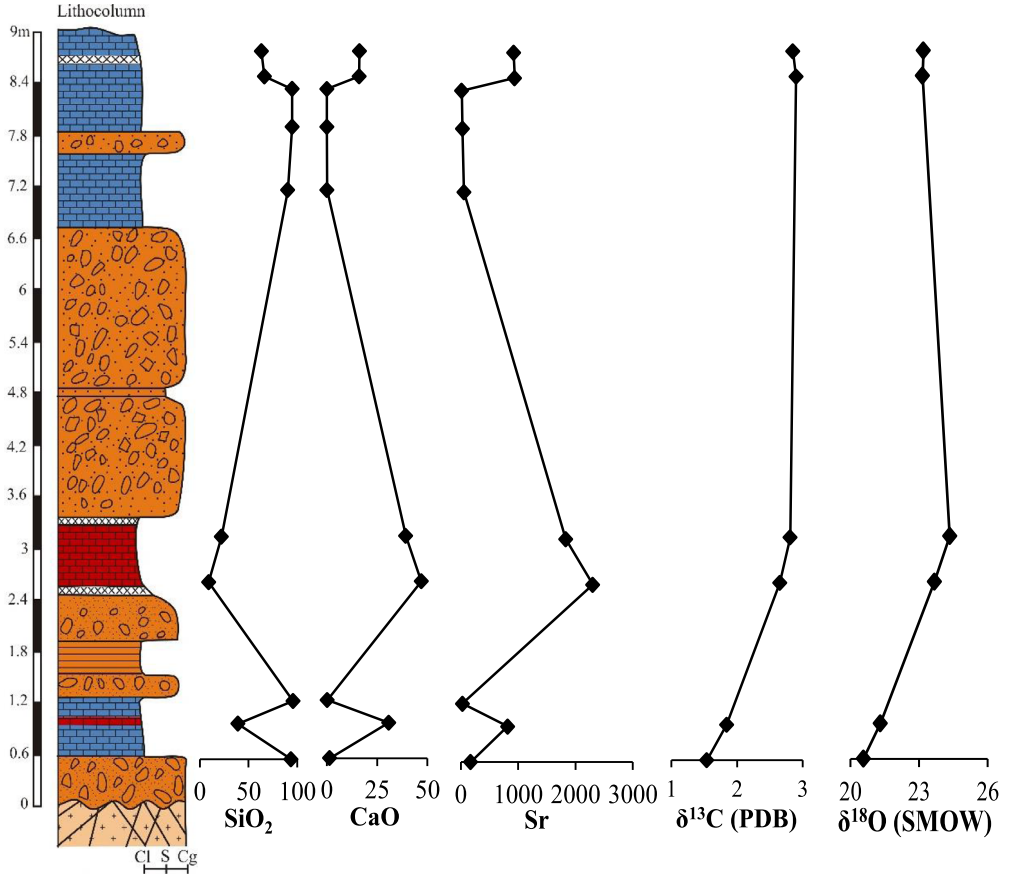

Supplementary Figure S4. Vertical variation of main chemical elements (SiO_2, CaO and Sr) and O and C isotope compositions from the main chemical deposits. (From bottom to top: TLT02, TLT0, TLT01, TLT1, TLT2, TLT3, TLAL, TLAS, TLAS2, TLTSB, TLTSV).

Supplementary Table S4. Stable carbon and oxygen isotope composition of Laopanga travertines, calcareo-siliceous sinters and siliceous sinters

Location	Facies types	Samples	$\delta^{13}C$ (‰ PDB)	$\delta^{18}O$ (‰ PDB)	$\delta^{18}O$ (‰ SMOW)	$\delta^{13}C$ parental CO_2 (Eq. 1) (‰ PDB)	$\delta^{13}C$ parental CO_2 (Eq. 2) (‰ PDB)
LAOPANGA	Travertines	TLT3	2.81	−6.37	24.34	−7.13	−16.21
		TLT2	2.42	−7.45	23.23	−7.59	−13.96
		TLT2b	2.73	−7.18	23.51	−7.22	−15.75
		TLT1	2.65	−7.02	23.67	−7.32	−15.29
		TLT01	1.84	−9.31	21.31	−8.29	−10.62
	Calcareo-siliceous sinters	TLTSB	2.9	−7.53	23.15	−7.02	−16.73
		TLTSV	2.85	−7.49	23.19	−7.08	−16.44
		TLTSVb	2.81	−7.41	23.27	−7.13	−16.21
	Siliceous sinters	TLT02	1.54	−10.03	20.57	−8.65	−8.88